

Review

Charge Transporting Materials Grown by Atomic Layer Deposition in Perovskite Solar Cells

Young Joon Cho , Min Ji Jeong, Ji Hye Park, Weiguang Hu , Jongchul Lim  and Hyo Sik Chang * 

Graduate School of Energy Science & Technology, Chungnam National University, Yuseong-gu, Daejeon 34134, Korea; jyj0317@nate.com (Y.J.C.); shmj0121@naver.com (M.J.J.); jihye50328@naver.com (J.H.P.); kaixinguo0121@hotmail.com (W.H.); jclim@cnu.ac.kr (J.L.)

* Correspondence: hschang@cnu.ac.kr; Tel.: +82-42-821-8607

Abstract: Charge transporting materials (CTMs) in perovskite solar cells (PSCs) have played an important role in improving the stability by replacing the liquid electrolyte with solid state electron or hole conductors and enhancing the photovoltaic efficiency by the efficient electron collection. Many organic and inorganic materials for charge transporting in PSCs have been studied and applied to increase the charge extraction, transport and collection, such as Spiro-OMeTAD for hole transporting material (HTM), TiO₂ for electron transporting material (ETM) and MoO_x for HTM etc. However, recently inorganic CTMs are used to replace the disadvantages of organic materials in PSCs such as, the long-term operational instability, low charge mobility. Especially, atomic layer deposition (ALD) has many advantages in obtaining the conformal, dense and virtually pinhole-free layers. Here, we review ALD inorganic CTMs and their function in PSCs in view of the stability and contribution to enhancing the efficiency of photovoltaics.

Keywords: perovskite; atomic layer deposition; charge transporting materials



Citation: Cho, Y.J.; Jeong, M.J.; Park, J.H.; Hu, W.; Lim, J.; Chang, H.S. Charge Transporting Materials Grown by Atomic Layer Deposition in Perovskite Solar Cells. *Energies* **2021**, *14*, 1156. <https://doi.org/10.3390/en14041156>

Academic Editor: Carlo Renno

Received: 4 January 2021

Accepted: 17 February 2021

Published: 22 February 2021

Publisher's Note: MDPI stays neutral with regard to jurisdictional claims in published maps and institutional affiliations.



Copyright: © 2021 by the authors. Licensee MDPI, Basel, Switzerland. This article is an open access article distributed under the terms and conditions of the Creative Commons Attribution (CC BY) license (<https://creativecommons.org/licenses/by/4.0/>).

1. Introduction

Presently, perovskite solar cells (PSCs) are one of the most outstanding devices using the solar cell technology, and their conversion efficiency has reached 25.5% in case of single-junction perovskite cells and 29.1% for perovskite/Si tandem cells [1]. Although PSCs have almost overtaken Si solar cells in terms of power conversion efficiency, the commercialization of PSCs is inhibited by several problems, such as the long-term stability and the large-scale fabrication issues. PSCs can be an alternative to the other solar cells if they are cheaper and more efficient with guaranteed long-term stability. Current manufacturers of photovoltaic (PV) modules provide a warranty for lost power replacement with power output of 90% after a decade and of 80% at the end of the warranty, which corresponds to less than 1% power loss per year [2]. The degradation of PSCs is known to be caused by oxygen and moisture, UV light, solution processing and thermal effects [3]. These factors react with the perovskite layers, such as the perovskite absorption layer, buffer layer, electron transporting layer (ETL) and hole transporting layer (HTL). This results in the decomposition of the perovskite absorber, non-stoichiometry defects, which are related to oxygen vacancies and titanium interstitials [4]. The traditional dye-sensitized solar cells (DSSCs) dye-sensitized and infiltrated a porous TiO₂ with a liquid electrolyte. This inherent instability in devices has been solved by replacing the liquid with the organic–inorganic metal halide materials, such as CH₃NH₃PbBr₃ and CH₃NH₃PbI₃ and as a result, the stability and the power conversion efficiency has been improved rapidly over a relatively short time. By replacing the liquid electrolyte with the organic–inorganic metal halide, the ETL and HTL have been investigated to reduce the degradation of organic ETL and HTL.

In this review, we focus the application and contribution of ALD to PSCs. First, in Section 2, we briefly describe the key materials and the historical background and development of PSCs and in Section 3, we describe the principle of ALD and its application

to PSCs. In Section 3, we discuss the CTMs grown by ALD for ETL and HTL. We conclude by summarizing PSCs and describing ALD issues.

2. Perovskite Solar Cells

Perovskites had been well-known in the scientific community for over a century before they were used as solar cell absorbers. The first natural perovskite was discovered by the mineralogist Gustav Rose in 1839 and perovskites, which have the chemical formula ABX_3 , adopt the same crystal structure as $CaTiO_3$. PSCs historically originate from DSSCs [5] and over decades the efficiency of PSCs has been enhanced considerably by the organic–inorganic metal halide materials. Metal halide perovskites have a direct band gap and strong light-absorption properties, high charge-carrier mobility, and small exciton binding energy [6]. These halide materials with the formula of ABX_3 consist of three ion parts, the organic cation (A), the metallic cation (B), and halide ion (X), as shown in Figure 1 [7]. Methylammonium $CH_3NH_3^+$, formamidinium $HC(NH_2)_2^+$ and cesium (Cs^+) are the materials used as the cations in perovskite absorbers and Pb^{2+} , Sn^{2+} , and Ge^{2+} are the metal cations. I^- , Cl^- , and Br^- are used as the halide ions. The combination of these materials shows various properties and solar cell performances [7–9]. Recently, organic–inorganic hybrid metal halides are emerging as perovskite absorber materials. But the structure and physical properties of $CH_3NH_3MX_3$, which is a type of perovskites, were first reported by Weber in 1978 [10] and these organic–inorganic perovskite materials, such as $(C_4H_9NH_3)_2(CH_3NH_3)_{n-1}Sn_nI_{3n+1}$, have been highlighted as high-temperature superconductor materials. These materials can be transformed into metal by inserting more inorganic layers; however, in the 1990s little attention was paid to them as solar cell absorbers [11].

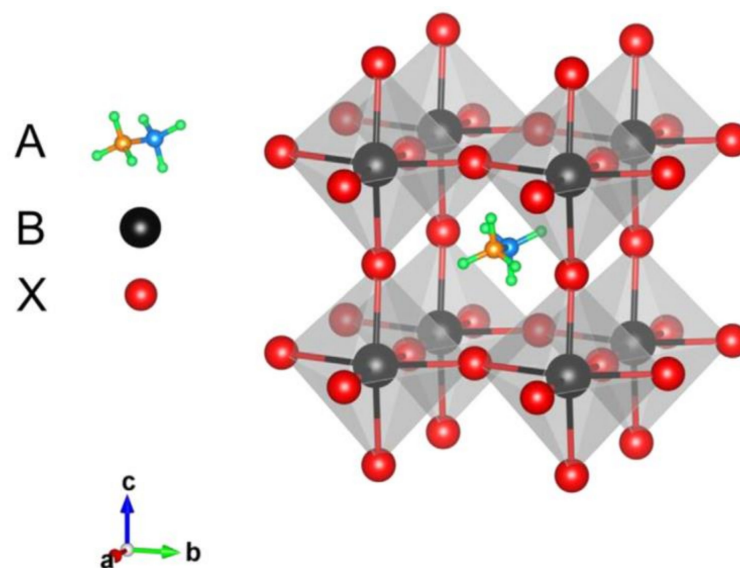


Figure 1. Crystal structure of an organic–inorganic metal halide perovskite. Reproduced with permission from Reference [7].

In 2006, Kojima presented the use of the perovskites, $CH_3NH_3PbBr_3$ as the sensitizer with 2.2% efficiency, in dye-sensitized cells at the 73rd Congress of the electrochemical Society of Japan at Tokyo Metropolitan University. Kojima et al. (2009) also reported PSCs using $CH_3NH_3PbBr_3$ and $CH_3NH_3PbI_3$ as absorbers and their PCEs were recorded 3.13% for the $CH_3NH_3PbI_3$ and 3.81% for the $CH_3NH_3PbBr_3$ -based devices, respectively [12]. However, owing to its low conversion efficiency and extreme instability, it could not be considered. Park et al. (2011) reported a 6.5% efficient PSC with $CH_3NH_3PbI_3$ absorber layer that had a little improved stability in electrolytes. However, the perovskite nanocrystals were dissolved in the iodide liquid electrolyte, which led to rapid device degradation, and it

only lasted approximately 10 min [13] and ever since the fabrication of the 9.7% solid-state PSCs with a 500 h long-term stability, the study of PSCs has become widespread [14].

PSCs sensitized the mesoporous TiO₂ layer with an organic–inorganic metal halide material such as methylammonium lead iodide CH₃NH₃PbI₃ (referred to as MAPbI₃) perovskite nanocrystals. The organic–inorganic metal halide material is an excellent light absorption material for PSCs. In terms of structure PSCs position the perovskite absorber between charge-transporting layers (CTLs) on a glass substrate. The light passes through the layers in the order ETL, perovskite absorber, and HTL from this glass referred to as n-i-p structure, a p-i-n structure has light pass through layers in the order HTL, perovskite absorber, and ETL. PSCs have two unique structures: a mesoscopic nanostructure and a planar structure. In a mesoscopic nanostructure PSC, the mesoporous Al₂O₃ and TiO₂ scaffold was infiltrated partially or completely by the perovskite materials.

Various organic and inorganic CTLs have been used in PSCs. Inorganic ETL materials comprise TiO₂, ZnO, SnO₂ and organic ETL materials include fullerene-based small molecular ETM, such as, [6,6]-Phenyl C61 Butyric acid Methyl ester (PCBM), and non-fullerene-based small molecular ETM, such as, a soluble perylene diimide (PDI) derivative, PDI-EH [15]. CTLs have been grown by spin coating, spray-pyrolysis, vacuum evaporation, chemical bath deposition, electro-deposition, and atomic layer deposition (ALD) [16]. In many growth methods, a thin charge selective layer is necessarily accompanied by the poor uniformity and conformality. These result in the decrease of carrier transporting and blocking characteristics, lowering the open-circuit voltage (V_{OC}), fill factor (FF), and reducing the long-term stability of solar cells. However, ALD can be a breakthrough to overcome this issue.

The solid contact was a prerequisite to enhance the PSCs stability because of polar iodine coming from iodine liquid electrolyte degraded the performance of PSCs. By mid-2012, a solid-state DSSCs was fabricated with exceptionally high PCE of 9.7% using spiro-OMeTAD as an HTM and a perovskite solar absorber (CH₃NH₃PbI₃) with a 500 h confirmed stability. The use of a solid-state HTM dramatically improved the stability of the device.

3. Atomic Layer Deposition (ALD)

The inorganic CTMs used in a PSC, have effective properties, such as, high hole mobility and low cost, e.g., CuI, CuSCN and NiO, but the solvent used for their deposition causes the perovskite to dissolve and degrade the device's stability [17]. ALD can be an alternative to solve the problem that is caused by the solution process, it is a piece of equipment used for depositing very thin and uniform films. ALD has good controllability, better step coverage, excellent stoichiometry, relatively low growth temperature, low impurity concentration and precise thickness control. For these reasons, ALD has a wide range of applicability, such as semiconductor, photovoltaics (PV), catalysis and biomaterials. The device downscaling in the semiconductor industry has greatly contributed to increasing the power conversion efficiency in PV with the ability to deposit the uniform Al₂O₃ passivation layer in crystalline Si solar cells.

The ALD process starts by injecting the metal precursor and oxidant pulse alternatively into the reaction chamber, as shown in Figure 2. Metal precursors and oxidant are adsorbed by surface chemical reactions on the substrate. This is followed by the purge steps which are inserted after the precursor and the oxidant pulse by injecting the inert gas, such as N₂ or Ar. ALD technique has been rapidly adopted in microelectronic device processes to deposit a wide variety of thin-film materials such as oxides, nitrides, and metals [18].

Metal oxides are grown by ALD, and these metal oxide films are used in many solar cells, such as c-Si, perovskite, heterojunction, and dye-sensitized solar cells as a surface passivation layer, buffer layer, absorber layer, electron/hole selective contact, or transparent conductive oxide. The ALD Al₂O₃ passivation layer began to be applied in c-Si solar cell, and the Al₂O₃ passivation layer increased the conversion efficiency, up to 23.2% in n-type Si solar cell [19].

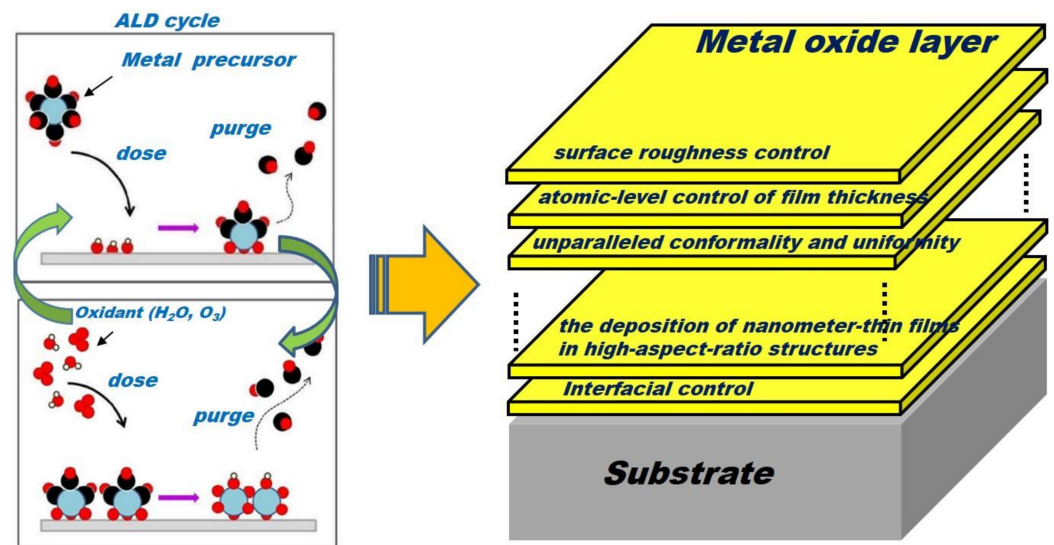


Figure 2. The schematic of atomic layer deposition (ALD) process and ALD characteristics.

4. Charge Transporting Materials (CTM) Grown by ALD

The charge separation and collection are very important to obtain a high-efficiency solar cell. A PSCs should overcome the degradation and dissolution of the absorbers by the solution process. ALD-CTM can be an alternative and has been studied for decades to avoid the degradation caused by the electrolyte solution. CTM must have several characteristics to collect electrons and block holes in the electrode and reduce the recombination loss. The ability of CTM in a solar cell depends on the alignment of energy level between the PSCs absorber and ETL or HTL (as shown in Figure 3). ETL (TiO_2 , ZnO , SnO_2) is required to have a conduction band minimum (CBM) aligned with or slightly lower than that of the PSCs absorber, transporting electrons and blocking holes. On the contrary, HTL (NiO and MoO_x) should have a shallower valence band maximum (VBM), for the VBM of the perovskite, extracting holes and blocking electrons, respectively (as shown in Figure 4).

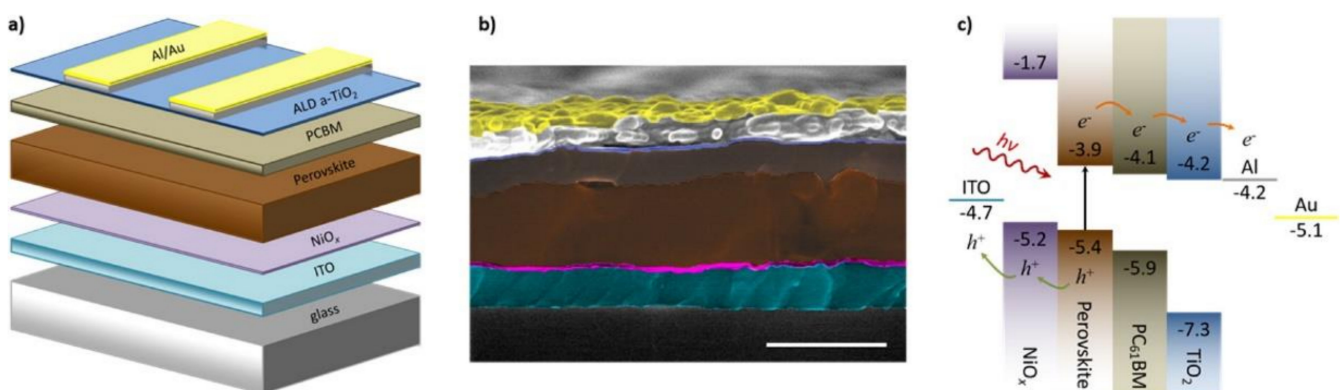


Figure 3. (a) Device architecture and (b) false color SEM image of the inverted perovskite photovoltaic device (scale bar 500 nm). (c) Idealized energy level diagram of the corresponding device architecture. Reproduced with permission from Reference [20].

4.1. Electron Transporting Materials

4.1.1. TiO_x

Lu et al. (2017) reported that a TiO_2 bilayer as an ETL in planar perovskite cells (FTO/spin-coating and ALD TiO_2 /perovskite/spiro-OMeTAD/Ag) was designed and fabricated by combining the ALD and spin-coating methods. Applying the TiO_2 bilayer as the ETL show enhanced FF, VOC, short circuit current density (JSC), and power conversion efficiency (PCE) compared with single layer-based cells.

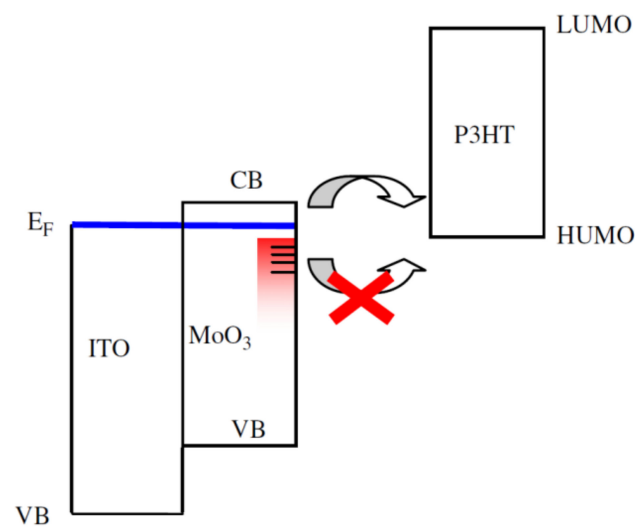


Figure 4. Schematics of charge extraction path ways at the anode buffer (MoO_3) and P3HT interface. Reproduced with permission from Reference [21].

The optimized spin-coating/ALD based devices show the highest PCEs of 16.5%. The excellent performance of the bilayer ETL based devices is caused by the improved carrier extraction, low charge transfer resistance, reduced recombination rate, and defect passivation [22]. Kim et al. (2015) fabricated highly efficient and bendable PSCs in a low-temperature process with a 20 nm-thick, low-impurity, amorphous TiO_x layer. The unaltered PEN/ TiO_x nanolayer/perovskite/spiro-OMeTAD multilayer shows that the bending durability of the TiO_x nanolayer-employed PSCs can be increased if that is achieved on the transparent conducting substrate [23]. However, effective TiO_2 electron selective layers (ESLs) usually are deposited in high-temperature processing, which is an obstacle for the commercialization of PSCs [24]. Although the electron transports from absorber to TiO_2 ETL are reported to be very fast, the TiO_2 layer cannot use this characteristic because of low electron mobility, which effectively raises the electron recombination loss at the interface [25,26]. Various reports have investigated zinc oxide (ZnO) as an alternative ETL because of better electron mobility than TiO_2 . However, ZnO suffers from inherent chemical instability, which can lower the long-term stability of the perovskite absorber [27]. TiO_2 was also reported to exhibit some limitations in the photovoltaics, such as low conductivity and a large number of defects, leading to the increase of carrier recombination rate [28]. This is also the reasons that the ZnO nanomaterials are paid attention in PbS colloidal quantum dots heterojunction photovoltaics [29].

4.1.2. ZnO

The resulting device of atomic layer deposited ZnO and Al_2O_3 films as a cathode buffer layer (CBL) and encapsulation layer with reflective opaque Ag electrode exhibited a remarkable PCE, up to 16.5% by combining low-temperature processed ($\leq 100^\circ\text{C}$) ALD ZnO with Al_2O_3 films as CBL and encapsulation layer into semitransparent (ST) PSCs, respectively [30].

ZnO is another commonly used ETM with a wide band gap and high electron mobility. However, ZnO has low chemical stability even when exposed to weak acids and bases [31] and it could easily react with perovskite in the thermal annealing condition of more than 100°C , which leads to the poor long-term stability of the devices [32].

4.1.3. Nb_2O_5

Subbiah et al. (2020) reported that ALD-grown Nb_2O_5 could serve as an alternative ETL with better stable power output than that of TiO_2 . A conformal Nb_2O_5 with 30 nm thickness using atomic layer deposition techniques with $\text{Nb}(\text{OEt})_5$ and H_2O was deposited on a fluorine-doped SnO_2 (FTO) substrate around 150°C . ALD- Nb_2O_5 shows a smooth

pinhole-free compact blocking layer in 3×3 cm area, which can be easily extended to the large-scale industrial manufacturing process. The amorphous ALD-Nb₂O₅ ETL-based perovskite devices offered device efficiencies of 14.2%, whereas the spin-coated crystalline Nb₂O₅ followed by annealing at 500 °C for 3 h showed highly resistive behavior with 1.5% efficiency. [27].

4.1.4. SnO_x

SnO_x as the ETL in the inverted solar cell stack was grown by ALD using tetrakisdimethylamino-Sn, Sn(N(CH₃)₂)₄ (TDMASn) as the Sn precursor. The cells with SnO_x show an efficiency of 3.4%, but it increases to 7.8% after consecutive JV sweeps, primarily due to an enhancing V_{OC}. Sn, O and halides are shown to be rich in perovskite/SnO_x interface. This is a possibility of nonideal chemical surface reactions during the ALD deposition and the current transport may be lowered [33]. Baena et al. (2015) demonstrated that planar PSCs employing the compact and pin-hole-free TiO₂ layer made by ALD exhibit a band misalignment and SnO₂ layer as ESL showed 1.19 V and 18% efficiency, respectively. The conduction band modification of the ESL could result in planar, high-performance PSCs with high voltages and good long-term stability. Furthermore, femtosecond transient absorption (TA) analysis clearly show that the mixed (FAP-bI₃)_{0.85}(MAPbBr₃)_{0.15} perovskite materials injected charges efficiently into SnO₂ but not into TiO₂ corroborating the conduction band misalignment at the TiO₂/perovskite interface. A barrier-free charge transport across the SnO₂/perovskite interface gives rise to the high and stable current densities—regardless of the sweep rate—which is not observed in TiO₂ based devices [34].

Wang et al. (2017) reported that the charge transport ability and electrical conductivity of SnO₂ ESLs grown by plasma-enhanced atomic layer deposition (PEALD) were increased after the annealing at 100 °C in H₂O ambient. As a result, V_{OC} and FF were improved and J–V hysteresis was reduced in PSCs using SnO₂ ESLs. Their flexible PSC showed a PCE of 18.36 (17.12)% measured under reverse (forward) voltage scan and a stabilized efficiency of over 17% using a commercial ITO/PET substrate [35]. Wang et al. have also reported that low-temperature PEALD SnO₂ ESLs has low electrical conductivity and can cause the degradation of charge transporting quality in PSCs and their planar PSC has recorded 20.3% PCE without antireflection coating [36].

Recent progress has suggested that SnO₂ is grown by PEALD below 100 °C as ETL [37] and highly efficient organic–inorganic metal-halide PSCs with a planar cell structure are fabricated as an excellent alternative to TiO₂, with enhanced bulk electron mobility, suitable band alignment, and high transparency (wide bandgap), resulting in highly efficient perovskite devices with reduced hysteresis [38,39].

4.2. Hole Transporting Materials

4.2.1. MoO_x

Recently Battaglia et al. (2014) introduced MoO_x ($x \approx 3$) as a promising candidate material, and it has already been applied successfully as hole selective contact in organic solar cells and PSCs [40–43]. The MoO_x is a suitable option for the replacement of p-type a-Si:H as hole selective layer owing to its high transparency, which can lead to a significant reduction in parasitic absorption. MoO_x has a much lower extinction coefficient and a higher band gap than a-Si:H (3.0 eV versus 1.7 eV). In addition, the refractive index of MoO_x is close to 2, which is ideal for light incoupling into the c-Si substrate. Although the mechanism of hole-selectivity of MoO_x is still under debate, it is perceived that the high work function of MoO_x of approximately 6.6 eV plays an important role and leads to an electronic band diagram that is similar to the conventional heterojunction with intrinsic thin layer (HIT) solar cell [44].

Jeong et al. (2019) reported that MoO_x film is deposited by ALD using molybdenum hexacarbonyl [Mo(CO)₆] as metal precursor and ozone (O₃) oxidant. The growth rate is about 0.036 nm/cycle and the thickness of interfacial oxide is approximately 2 nm. The band gap and work function are 3.25 eV and 8 eV, respectively. By applying ALD-MoO_x

layer instead of the p-type a-Si layer in the HIT solar cell, similar results to HIT cell were shown in lifetime and implied V_{OC} , as shown in Figure 5, and the power conversion efficiency reached 21.06% and V_{OC} 726 mV, J_{SC} 38.5 mA/cm², FF 75.1%, as shown in Figure 6 [45].

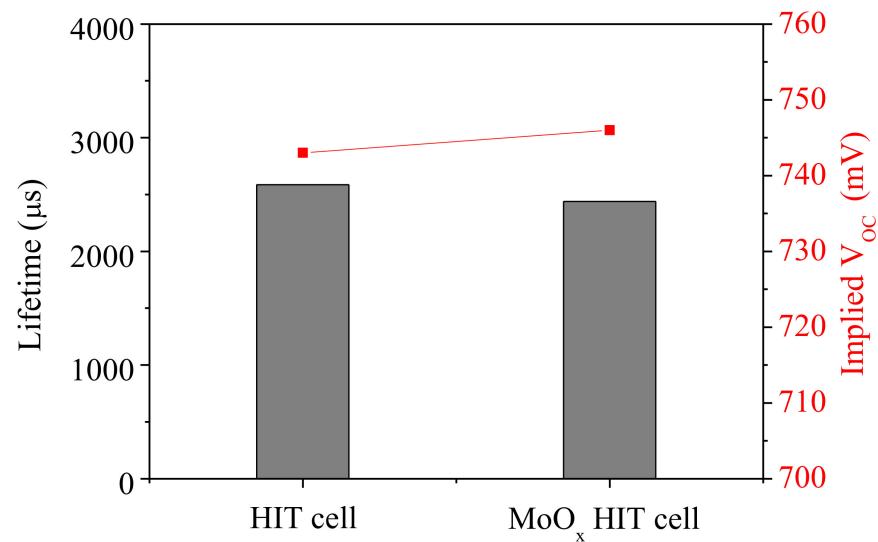


Figure 5. Change of effective carrier lifetime and implied V_{OC} before and after MoO_x application to HIT cell. Reproduced with permission from Reference [45].

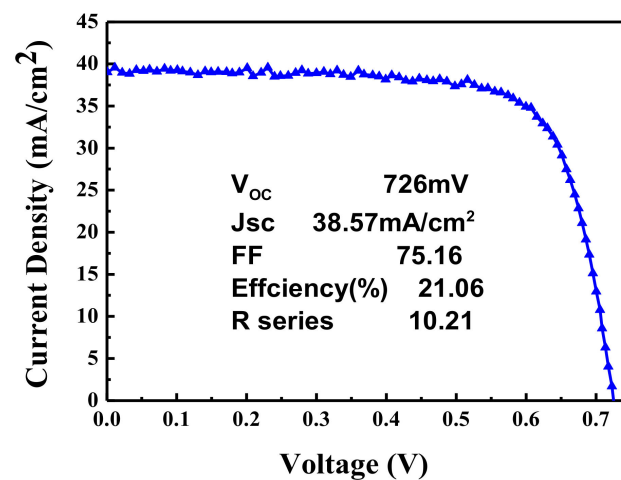


Figure 6. I–V Curve for the ALD-MoO_x applied HIT cell. Reproduced with permission from Reference [45].

4.2.2. WO_x

Tungsten oxides (WO_x) have wide bandgaps (2 to 3 eV) [46,47] and higher electron mobility (10–20 cm²·V⁻¹·s⁻¹) and are chemically stable [48,49]. These excellent properties enable the efficient extraction of photogenerated electrons to electrode. Very recently, WO_x ETL was prepared for PSCs via high-temperature annealing, and a WO_x–TiO₂ core–shell nanostructure was applied to decrease charge recombination rate at the perovskite/WO_x interface [50].

4.2.3. VO_x

Chu et al. reported that ultra-thin VO_x layer was grown at the low temperature of 50 °C and can be one of the candidates of HTL for PSCs. After UV post-treatment, ALD-VO_x showed 11.53% efficiency by enhancing hole transporting characteristic. The interface

energy band bending was preferred for the FTO-VO_x-UV/MAPbI₃ interface, thereby enhancing the hole transport across the interface [51].

To investigate the passivation characteristic of VO_x, it was grown by ALD on an n-type Si solar wafer, and the lifetime and implied V_{OC} were measured by QSSPC. Vanadium triisopropoxide (VTIP) was used as a metal precursor and H₂O as an oxidant, and its growth rate was 0.016 nm/cycle. As shown in Figure 7, the implied V_{OC} was raised by about 20 mV, compared to that of the thermal evaporated VO_x [52]. After post-annealing for 30 min in ambient N₂, the lifetime and implied V_{OC} was improved by 20 μs; and 10 mV owing to the decrease of carbon content in ALD-VO_x film [53].

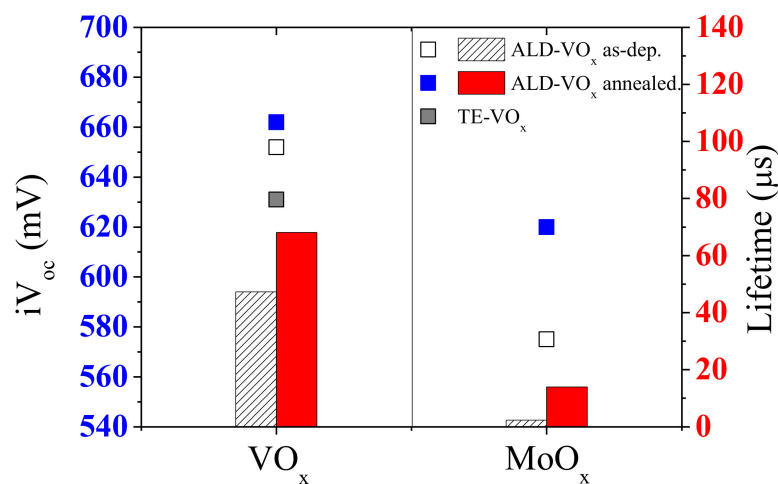


Figure 7. The comparison of lifetime and implied V_{OC} for as-dep and annealed ALD-VO_x and thermal evaporated VO_x. Reproduced with permission from Reference [53].

4.2.4. NiO_x

Koushik et al. (2019) reported that a plasma-assisted ALD-NiO thin film has been grown using Ni(MeCp)₂ as metal precursor and O₂ plasma as oxidant. The polycrystalline, cubic 10 nm NiO films as HTL with 3.75 eV bandgap is deposited, and the ALD-NiO layers recorded 17.07% PCE after post-annealing. Hole transporting quality is improved and as a result, J_{SC} and FF increased. This improvement is attributed to enhanced wetting of the perovskite layer atop. The electrical conductivity and charge mobility of NiO are also increased after post-annealing [54].

5. Conclusions and Perspectives

This review article focuses on the historical progress of PSCs and the contribution of ALD to PSCs. Over the decades, the study of PSCs have improved the efficiency of PSCs to be competitive to that of Si solar cells, but there are still several obstacles that inhibit commercialization, such as the long-term stability. The degradation mechanism of PSCs needs to be understood to overcome these obstacles. From this perspective, ALD has advantages and can be an excellent alternative to solution processes, such as spin coating, spray pyrolysis, and chemical bath deposition. The long-term stability issue has been overcome by ALD-grown inorganic CTLs and the absorber layer grown by a vacuum process, replacing the solution process. Although ALD has recently been applied and contributed to PSCs development, it is still a minor growth method, compared to the solution process. In addition, the carbon content in the CTL films should be reduced at low-temperature deposition during the ALD process. Direct oxide-CTL deposition using ALD on perovskite film is difficult owing to the deterioration of the perovskite film.

An interlayer is required between perovskite and ALD-CTL. Direct oxide-CTL deposition using ALD on perovskite films requires that the ALD deposition temperature be maintained below 60 °C to prevent degradation of perovskite properties. The architecture of the PSCs and the application of CTLs and their properties is summarized in Table 1.

Table 1. The summary of charge-transporting layers (CTL) and their properties.

Device Design/Architecture	Bandgap/eV	Refractive Index	J _{sc} /mAcm ⁻²	V _{oc} /V	FF/%	PCE/%	Active Area/cm ²	Ref
FTO/spin coated TiO ₂ /ALD TiO ₂ (10 nm)/perovskite/Spiro-OMeTAD/Ag	3.2	2.6	20.5 ± 0.17	1.07 ± 0.014	75.2 ± 0.80	16.5 ± 0.44	0.15	[21]
ITO/PEDOT:PSS/perovskite/ALD ZnO/Ag NWs	3.2	2	20.73 ± 0.79	1.02 ± 0.01	76.36 ± 3.02	16.15 ± 0.20	0.04	[28]
FTO/ALD-Nb ₂ O ₅ /MAPbI ₃ /Spiro-OMeTAD/Au(Backward)	3.4	2.3	21.7	1.013	70	15.4	0.12	[25]
glass/fluorine doped SnO ₂ (FTO)/PEALD-SnO ₂ /fullerene self-assembled monolayer (C ₆₀ -SAM)/MA _{0.7} FA _{0.3} PbI ₃ /Spiro-OMeTAD/Au	3.5	2.3–2.8	22.61	1.125	79.77	20.29	0.08	[34]
FTO/VOx/perovskite/phenyl-C ₆₁ -butyric acid methyl ester(PCBM)/bathocuproine (BCP)/Ag	3.6	1.6–2.3	17.58	0.87	66.41	10.17	0.1	[49]
glass substrate/ITO/ALD NiO/perovskite/C ₆₀ /BCP (bathocuproine)/Cu, inverted (p–i–n) planar structure	3.5	2.1	21.75	1.05	73.36	17.07	0.86	[52]
FTO/TiO ₂ /CH ₃ NH ₃ PbI ₃ /Spiro-OMeTAD/MoOx/Metal (Ag or Al)	3.25	2.1	20.14	0.993	0.602	12.04	0.2–0.3	[40]
FTO/WO _x /MAPbI _x Cl _{3-x} /Spiro-OMeTAD/Ag	3.15	3.9	21.77 ± 1.04	0.71 ± 0.03	0.58 ± 0.02	8.99 ± 0.41	0.06	[48]

In the future, if the dissolution and degradation of the PSCs absorber layer by the solution process are removed by ALD, ALD-metal oxide will be a remarkable breakthrough for commercialization, similar to the contribution of ALD-Al₂O₃ as the passivation layer to Si solar cell and ALD CTLs are promising for silicon–perovskite tandem solar cells.

Author Contributions: Conceptualization, H.S.C.; methodology, M.J.J., J.H.P., W.H., and Y.J.C.; writing—original draft preparation, Y.J.C.; writing—review and editing, Y.J.C., J.L. and H.S.C.; supervision, H.S.C. All authors have read and agreed to the published version of the manuscript.

Funding: This research received no external funding.

Institutional Review Board Statement: Not applicable.

Informed Consent Statement: Not applicable.

Data Availability Statement: Not applicable.

Acknowledgments: This work was supported by research fund of Chungnam National University.

Conflicts of Interest: The authors declare no conflict of interest.

References

- NREL. Best Research Efficiency. Available online: <https://www.nrel.gov/pv/assets/pdfs/best-research-cell-efficiencies.20210104.pdf> (accessed on 14 February 2020).
- Roesch, R.; Faber, T.; Von Hauff, E.; Brown, T.M.; Lira-Cantu, M.; Hoppe, H. Procedures and practices for evaluating thin-film solar cell stability. *Adv. Energy Mater.* **2015**, *5*, 1501407. [CrossRef]
- Niu, G.; Guo, X.; Wang, L. Review of recent progress in chemical stability of perovskite solar cells. *J. Mater. Chem. A* **2015**, *3*, 8970–8980. [CrossRef]
- Pathak, S.K.; Abate, A.; Ruckdeschel, P.; Roose, B.; Gödel, K.C.; Vaynzof, Y.; Santhala, A.; Watanabe, S.-I.; Hollman, D.J.; Noel, N.; et al. Performance and Stability Enhancement of Dye-Sensitized and Perovskite Solar Cells by Al Doping of TiO₂. *Adv. Funct. Mater.* **2014**, *24*, 6046–6055. [CrossRef]
- Grätzel, M. The light and shade of perovskite solar cells. *Nat. Mater.* **2014**, *13*, 838–842. [CrossRef]
- Calió, L.; Kazim, S.; Grätzel, M.; Ahmad, S. Hole-Transport Materials for Perovskite Solar Cells. *Angew. Chem. Int. Ed.* **2016**, *55*, 14522–14545. [CrossRef]
- Wang, D.; Wright, M.; Elumalai, N.K.; Uddin, A. Stability of perovskite solar cells. *Sol. Energy Mater. Sol. Cells* **2016**, *147*, 255–275. [CrossRef]

8. Zuo, C.; Bolink, H.J.; Han, H.; Huang, J.; Cahen, D.; Ding, L. Advances in Perovskite Solar Cells. *Adv. Sci.* **2016**, *3*, 1500324. [[CrossRef](#)]
9. Wehrenfennig, C.; Eperon, G.E.; Johnston, M.B.; Snaith, H.J.; Herz, L.M. High Charge Carrier Mobilities and Lifetimes in Organolead Trihalide Perovskites. *Adv. Mater.* **2014**, *26*, 1584–1589. [[CrossRef](#)]
10. Weber, D. $\text{CH}_3\text{NH}_3\text{PbX}_3$, ein Pb(II)-System mit kubischer Perowskitstruktur / $\text{CH}_3\text{NH}_3\text{PbX}_3$, a Pb(II)-System with Cubic Perovskite Structure. *Z. Naturforsch. B* **1978**, *33*, 1443–1445. [[CrossRef](#)]
11. Mitzi, D.B.; Feild, C.A.; Harrison, W.T.A.; Guloy, A.M. Conducting tin halides with a layered organic-based perovskite structure. *Nature* **1994**, *369*, 467–469. [[CrossRef](#)]
12. Green, M.A.; Ho-Baillie, A. Perovskite Solar Cells: The Birth of a New Era in Photovoltaics. *ACS Energy Lett.* **2017**, *2*, 822–830. [[CrossRef](#)]
13. Im, J.-H.; Lee, C.-R.; Lee, J.-W.; Park, S.-W.; Park, N.-G. 6.5% efficient perovskite quantum-dot-sensitized solar cell. *Nanoscale* **2011**, *3*, 4088. [[CrossRef](#)]
14. Kim, H.-S.; Lee, C.-R.; Im, J.-H.; Lee, K.-B.; Moehl, T.; Marchioro, A.; Moon, S.-J.; Humphry-Baker, R.; Yum, J.-H.; Moser, J.E.; et al. Lead Iodide Perovskite Sensitized All-Solid-State Submicron Thin Film Mesoscopic Solar Cell with Efficiency Exceeding 9%. *Sci. Rep.* **2012**, *2*, 591. [[CrossRef](#)]
15. Zhang, W.; Wang, Y.-C.; Li, X.; Song, C.; Wan, L.; Usman, K.; Fang, J. Recent Advance in Solution-Processed Organic Interlayers for High-Performance Planar Perovskite Solar Cells. *Adv. Sci.* **2018**, *5*, 1800159. [[CrossRef](#)]
16. Wang, K.; Olthof, S.; Subhani, W.S.; Jiang, X.; Cao, Y.; Duan, L.; Wang, H.; Du, M.; Liu, S. (Frank) Novel inorganic electron transport layers for planar perovskite solar cells: Progress and prospective. *Nano Energy* **2020**, *68*, 104289. [[CrossRef](#)]
17. Qin, P.; Tanaka, S.; Ito, S.; Tetreault, N.; Manabe, K.; Nishino, H.; Nazeeruddin, M.K.; Grätzel, M. Inorganic hole conductor-based lead halide perovskite solar cells with 12.4% conversion efficiency. *Nat. Commun.* **2014**, *5*, 3834. [[CrossRef](#)]
18. An, K.S.; Cho, W.; Sung, K.; Lee, S.S.; Kim, Y. Preparation of Al_2O_3 Thin Films by Atomic Layer Deposition Using Dimethylaluminum Isopropoxide and Water and Their Reaction Mechanisms. *Bull. Korean Chem. Soc.* **2003**, *24*, 1659–1663. [[CrossRef](#)]
19. Benick, J.; Hoex, B.; van de Sanden, M.C.M.; Kessels, W.M.M.; Schultz, O.; Glunz, S.W. High efficiency n-type Si solar cells on Al_2O_3 -passivated boron emitters. *Appl. Phys. Lett.* **2008**, *92*, 253504. [[CrossRef](#)]
20. Kim, I.S.; Cao, D.H.; Buchholz, D.B.; Emery, J.D.; Farha, O.K.; Hupp, J.T.; Kanatzidis, M.G.; Martinson, A.B.F. Liquid Water- and Heat-Resistant Hybrid Perovskite Photovoltaics via an Inverted ALD Oxide Electron Extraction Layer Design. *Nano Lett.* **2016**, *16*, 7786–7790. [[CrossRef](#)]
21. Chiam, S.Y.; Dasgupta, B.; Soler, D.; Leung, M.Y.; Liu, H.; Ooi, Z.E.; Wong, L.M.; Jiang, C.Y.; Chang, K.L.; Zhang, J. Investigating the stability of defects in MoO_3 and its role in organic solar cells. *Sol. Energy Mater. Sol. Cells* **2012**, *99*, 197–203. [[CrossRef](#)]
22. Lu, H.; Tian, W.; Gu, B.; Zhu, Y.; Li, L. TiO_2 Electron Transport Bilayer for Highly Efficient Planar Perovskite Solar Cell. *Small* **2017**, *13*, 1701535. [[CrossRef](#)]
23. Kim, B.J.; Kim, D.H.; Lee, Y.-Y.; Shin, H.-W.; Han, G.S.; Hong, J.S.; Mahmood, K.; Ahn, T.K.; Joo, Y.-C.; Hong, K.S.; et al. Highly efficient and bending durable perovskite solar cells: Toward a wearable power source. *Energy Environ. Sci.* **2015**, *8*, 916–921. [[CrossRef](#)]
24. Yang, G.; Lei, H.; Tao, H.; Zheng, X.; Ma, J.; Liu, Q.; Ke, W.; Chen, Z.; Xiong, L.; Qin, P.; et al. Reducing Hysteresis and Enhancing Performance of Perovskite Solar Cells Using Low-Temperature Processed Y-Doped SnO_2 Nanosheets as Electron Selective Layers. *Small* **2017**, *13*, 1601769. [[CrossRef](#)]
25. Mahmood, K.; Sarwar, S.; Mehran, M.T. Current status of electron transport layers in perovskite solar cells: Materials and properties. *RSC Adv.* **2017**, *7*, 17044–17062. [[CrossRef](#)]
26. Yang, G.; Tao, H.; Qin, P.; Ke, W.; Fang, G. Recent progress in electron transport layers for efficient perovskite solar cells. *J. Mater. Chem. A* **2016**, *4*, 3970–3990. [[CrossRef](#)]
27. Subbiah, A.S.; Dhara, A.K.; Mahuli, N.; Banerjee, S.; Sarkar, S.K. Ultra-Thin Atomic Layer Deposited- Nb_2O_5 as Electron Transport Layer for Co-Evaporated MAPbI₃ Planar Perovskite Solar Cells. *Energy Technol.* **2020**, *8*, 1900878. [[CrossRef](#)]
28. Zhu, Y.; Deng, K.; Sun, H.; Gu, B.; Lu, H.; Cao, F.; Xiong, J.; Li, L. TiO_2 Phase Junction Electron Transport Layer Boosts Efficiency of Planar Perovskite Solar Cells. *Adv. Sci.* **2018**, *5*, 1700614. [[CrossRef](#)]
29. Zeng, T.; Su, X.; Feng, S.; Xie, Y.; Chen, Y.; Shen, Z.; Shi, W. Thermally-stable hydroxyl radicals implanted on TiO_2 electron transport layer for efficient carrier extraction in PbS quantum dot photovoltaics. *Sol. Energy Mater. Sol. Cells* **2018**, *188*, 263–272. [[CrossRef](#)]
30. Chang, C.-Y.; Lee, K.-T.; Huang, W.-K.; Siao, H.-Y.; Chang, Y.-C. High-Performance, Air-Stable, Low-Temperature Processed Semitransparent Perovskite Solar Cells Enabled by Atomic Layer Deposition. *Chem. Mater.* **2015**, *27*, 5122–5130. [[CrossRef](#)]
31. Wali, Q.; Iqbal, Y.; Pal, B.; Lowe, A.; Jose, R. Tin oxide as an emerging electron transport medium in perovskite solar cells. *Sol. Energy Mater. Sol. Cells* **2018**, *179*, 102–117. [[CrossRef](#)]
32. Yang, J.; Siempelkamp, B.D.; Mosconi, E.; De Angelis, F.; Kelly, T.L. Origin of the Thermal Instability in $\text{CH}_3\text{NH}_3\text{PbI}_3$ Thin Films Deposited on ZnO. *Chem. Mater.* **2015**, *27*, 4229–4236. [[CrossRef](#)]
33. Hultqvist, A.; Aitola, K.; Sveinbjörnsson, K.; Saki, Z.; Larsson, F.; Törndahl, T.; Johansson, E.; Boschloo, G.; Edoff, M. Atomic Layer Deposition of Electron Selective SnO_x and ZnO Films on Mixed Halide Perovskite: Compatibility and Performance. *ACS Appl. Mater. Interfaces* **2017**, *9*, 29707–29716. [[CrossRef](#)]

34. Correa Baena, J.P.; Steier, L.; Tress, W.; Saliba, M.; Neutzner, S.; Matsui, T.; Giordano, F.; Jacobsson, T.J.; Srimath Kandada, A.R.; Zakeeruddin, S.M.; et al. Highly efficient planar perovskite solar cells through band alignment engineering. *Energy Environ. Sci.* **2015**, *8*, 2928–2934. [[CrossRef](#)]
35. Wang, C.; Guan, L.; Zhao, D.; Yu, Y.; Grice, C.R.; Song, Z.; Awni, R.A.; Chen, J.; Wang, J.; Zhao, X.; et al. Water Vapor Treatment of Low-Temperature Deposited SnO₂ Electron Selective Layers for Efficient Flexible Perovskite Solar Cells. *ACS Energy Lett.* **2017**, *2*, 2118–2124. [[CrossRef](#)]
36. Wang, C.; Xiao, C.; Yu, Y.; Zhao, D.; Awni, R.A.; Grice, C.R.; Ghimire, K.; Constantinou, I.; Liao, W.; Cimaroli, A.J.; et al. Understanding and Eliminating Hysteresis for Highly Efficient Planar Perovskite Solar Cells. *Adv. Energy Mater.* **2017**, *7*, 1700414. [[CrossRef](#)]
37. Wang, C.; Zhao, D.; Grice, C.R.; Liao, W.; Yu, Y.; Cimaroli, A.; Shrestha, N.; Roland, P.J.; Chen, J.; Yu, Z.; et al. Low-temperature plasma-enhanced atomic layer deposition of tin oxide electron selective layers for highly efficient planar perovskite solar cells. *J. Mater. Chem. A* **2016**, *4*, 12080–12087. [[CrossRef](#)]
38. Anaraki, E.H.; Kermanpur, A.; Steier, L.; Domanski, K.; Matsui, T.; Tress, W.; Saliba, M.; Abate, A.; Grätzel, M.; Hagfeldt, A.; et al. Highly efficient and stable planar perovskite solar cells by solution-processed tin oxide. *Energy Environ. Sci.* **2016**, *9*, 3128–3134. [[CrossRef](#)]
39. Dong, Q.; Shi, Y.; Wang, K.; Li, Y.; Wang, S.; Zhang, H.; Xing, Y.; Du, Y.; Bai, X.; Ma, T. Insight into Perovskite Solar Cells Based on SnO₂ Compact Electron-Selective Layer. *J. Phys. Chem. C* **2015**, *119*, 10212–10217. [[CrossRef](#)]
40. Tseng, Y.; Mane, A.U.; Elam, J.W.; Darling, S.B. Ultrathin molybdenum oxide anode buffer layer for organic photovoltaic cells formed using atomic layer deposition. *Sol. Energy Mater. Sol. Cells* **2012**, *99*, 235–239. [[CrossRef](#)]
41. Bullock, J.; Cuevas, A.; Allen, T.; Battaglia, C. Molybdenum oxide MoO_x: A versatile hole contact for silicon solar cells. *Appl. Phys. Lett.* **2014**, *105*, 232109. [[CrossRef](#)]
42. Battaglia, C.; de Nicolás, S.M.; De Wolf, S.; Yin, X.; Zheng, M.; Ballif, C.; Javey, A. Silicon heterojunction solar cell with passivated hole selective MoO_x contact. *Appl. Phys. Lett.* **2014**, *104*, 113902. [[CrossRef](#)]
43. Niu, W.; Li, X.; Karuturi, S.K.; Fam, D.W.; Fan, H.; Shrestha, S.; Wong, L.H.; Tok, A.I.Y. Applications of atomic layer deposition in solar cells. *Nanotechnology* **2015**, *26*, 064001. [[CrossRef](#)]
44. Vos, M.F.J. Atomic Layer Deposition of Molybdenum Oxide for Silicon Heterojunction Solar Cells. Master's Thesis, TU/e Eindhoven University of Technology, Eindhoven, The Netherlands, 2015. Available online: <https://research.tue.nl/en/studentTheses/atomic-layer-deposition-of-molybdenum-oxide> (accessed on 14 February 2021).
45. Jeong, M.J.; Jo, Y.J.; Lee, S.H.; Lee, J.S.; Im, K.J.; Seo, J.H.; Chang, H.S. Heterojunction Solar Cell with Carrier Selective Contact Using MoO_x Deposited by Atomic Layer Deposition. *Korean J. Mater. Res.* **2019**, *29*, 322–327. [[CrossRef](#)]
46. Washizu, E. Optical and electrochromic properties of RF reactively sputtered WO₃ films. *Solid State Ion.* **2003**, *165*, 175–180. [[CrossRef](#)]
47. Ottaviano, L.; Lozzi, L.; Passacantando, M.; Santucci, S. On the spatially resolved electronic structure of polycrystalline WO₃ films investigated with scanning tunneling spectroscopy. *Surf. Sci.* **2001**, *475*, 73–82. [[CrossRef](#)]
48. Weinhardt, L.; Blum, M.; Bär, M.; Heske, C.; Cole, B.; Marsen, B.; Miller, E.L. Electronic Surface Level Positions of WO₃ Thin Films for Photoelectrochemical Hydrogen Production. *J. Phys. Chem. C* **2008**, *112*, 3078–3082. [[CrossRef](#)]
49. Gillet, M.; Aguir, K.; Lemire, C.; Gillet, E.; Schierbaum, K. The structure and electrical conductivity of vacuum-annealed WO₃ thin films. *Thin Solid Films* **2004**, *467*, 239–246. [[CrossRef](#)]
50. Wang, K.; Shi, Y.; Dong, Q.; Li, Y.; Wang, S.; Yu, X.; Wu, M.; Ma, T. Low-Temperature and Solution-Processed Amorphous WO_x as Electron-Selective Layer for Perovskite Solar Cells. *J. Phys. Chem. Lett.* **2015**, *6*, 755–759. [[CrossRef](#)]
51. Chu, S.; Zhao, R.; Liu, R.; Gao, Y.; Wang, X.; Liu, C.; Chen, J.; Zhou, H. Atomic-layer-deposited ultra-thin VO_x film as a hole transport layer for perovskite solar cells. *Semicond. Sci. Technol.* **2018**, *33*, 115016. [[CrossRef](#)]
52. Gerling, L.G.; Mahato, S.; Morales-Vilches, A.; Masmitja, G.; Ortega, P.; Voz, C.; Alcubilla, R.; Puigdollers, J. Transition metal oxides as hole-selective contacts in silicon heterojunctions solar cells. *Sol. Energy Mater. Sol. Cells* **2016**, *145*, 109–115. [[CrossRef](#)]
53. Park, J.; Chang, H.S. Characteristics of Vanadium Oxide Grown by Atomic Layer Deposition for Hole Carrier Selective Contacts Si Solar Cells. *Korean J. Mater. Res.* **2020**, *30*, 660–665. [[CrossRef](#)]
54. Koushik, D.; Jošt, M.; Dučinskis, A.; Burgess, C.; Zardetto, V.; Weijtens, C.; Verheijen, M.A.; Kessels, W.M.M.; Albrecht, S.; Creatore, M. Plasma-assisted atomic layer deposition of nickel oxide as hole transport layer for hybrid perovskite solar cells. *J. Mater. Chem. C* **2019**, *7*, 12532–12543. [[CrossRef](#)]